Signatures of motor susceptibility to forces in the dynamics of a tracer particle in an active gel

Nitzan Razin,[1] Raphael Voituriez,[2] and Nir S. Gov[1]

[1]*Department of Chemical and Biological Physics, Weizmann Institute of Science, Rehovot 76100, Israel*

[2]*Laboratoire Jean Perrin and Laboratoire de Physique Théorique de la Matière Condensée, CNRS / Sorbonne Universite, 75005 Paris, France*

(Received 22 June 2018; revised manuscript received 5 January 2019; published 25 February 2019)

We study a model for the motion of a tracer particle inside an active gel, exposing the properties of the van Hove distribution of the particle displacements. Active events of a typical force magnitude can give rise to non-Gaussian distributions having exponential tails or side peaks. The side peaks are predicted to appear when the local bulk elasticity of the gel is large enough and few active sources are dominant. We explain the regimes of the different distributions and study the structure of the side peaks for active sources that are susceptible to the elastic stress that they cause inside the gel. We show how the van Hove distribution is altered by both the duty cycle of the active sources and their susceptibility, and suggest it as a sensitive probe to analyze microrheology data in active systems with restoring elastic forces.

DOI: 10.1103/PhysRevE.99.022419

I. INTRODUCTION

Active gels, composed of a cross-linked network of biopolymers that contains molecular motors which produce active forces, are *in vitro* model systems for exploring nonequilibrium physics as well as studying the dynamics inside living cells [1–14]. The dynamics of an active gel can be probed experimentally by following the displacements of a passive tracer particle [6–9]. The time-dependent distribution of the displacements, the van Hove distribution (VHD), was observed to be an indicator of activity inside the gel, exhibiting distinct non-Gaussian form in the presence of activity [6–8]. The active gels in these *in vitro* experiments [6–9] consist of cross-linked actin filaments and bundles, which are furthermore perfused by myosin-II molecular motors. When chemical energy is supplied (in the form of Adenosine triphosphate (ATP)), the motors become active and give rise to contractile forces that are applied locally to the actin filaments. Note that in many experiments [6–8] these forces induce strong evolution of the network, until it collapses. In Ref. [9] smaller motor bundles were used in order to achieve a more stable steady-state system. It was further predicted theoretically that when the motion is dominated by a few sources of active forces, and the elastic stiffness of the gel is high, there should appear side peaks in the VHD [14]. This peak structure arises from the discrete displacement of the tracer particle due to the force balance between the active force and the elastic restoring force, but this has not yet been observed in experiments.

In this paper, we study how the VHD changes with the properties of the active forces. We show that the model introduced in Ref. [14] has parameter regimes where the VHD has exponential tails, similar to those commonly measured for tracers in active gels [6–8]. We then introduce and explore the effects of susceptibility of the active sources to the elastic stress in the active gel, which is itself produced by the activity. This is motivated by the known susceptibility of molecular motors, such as myosin-II, to applied forces, which modify their kinetics [15–20], and it is therefore an essential feature to include in a realistic model of active gels. We reveal how the susceptibility of the motors affects the peak structure in the VHD, thereby demonstrating that it is a sensitive probe for the properties of the active sources inside active gels and living cells. Our results may be relevant to many active systems with restoring elastic forces, such as artificial active membranes [21–23], cellular membranes [24], active polymers [25–27], particles within optical traps [28], dense active fluids [29–31], and active fluctuations observed in the chromatin in the nucleus of living cells [32–36].

II. MODEL DEFINITION

We start by studying a one-dimensional model for the motion of a tracer particle in the active gel, which was introduced in Ref. [14]. The particle is trapped in a harmonic potential $U(x) = \frac{1}{2}kx^2$, representing the bulk elasticity of the gel. This description is valid at short times, in which the particle is trapped, since at long times the actin network reorganizes and the particle performs free diffusion [6,9]. In addition, the particle moves due to the force applied by N "motors," each representing a source of active events which applies a force with typical magnitude F_0 for an exponentially distributed time duration with average $k_{\rm off}^{-1}$. At first we assume that the motors are independent and identically distributed: each of them can be either on or off. When a motor is off, it does not apply any force to the particle. The motor turns on after an exponentially distributed duration, with rate $k_{\rm on}$. Once the motor is on, a direction (left or right) is randomly chosen and the motor applies a force of magnitude F_0 in that direction to the particle.

The Langevin equation of motion for the particle position x is thus

$$m\ddot{x} = -\gamma\dot{x} - kx - \sum_{i=1}^{N} M_i(t)F_0 + \xi(t), \tag{1}$$

where m is the particle mass, γ is a friction coefficient, and M_i is a variable representing the state of the ith motor which is equal to 0 when the motor is off and ± 1 when the motor is on in the right/left direction. $\xi(t)$ is white noise that can be of thermal or other origin (such as activity from many sources that are far from the particle). We neglect ξ, since small white noise does not significantly affect the properties of the VHD peak structure in which we are interested. Moreover, in cellular systems active temperatures are usually much larger than thermal ones. The motion of tracer particles in cellular systems and artificial active gels is typically overdamped. Accordingly, our model focuses on this regime, where the friction timescale m/γ is smaller than the other timescales, k_{off}^{-1}, k_{on}^{-1}, and γ/k. Yet we keep the general form of the Langevin equation in all of our simulations for accuracy and consistency, since as the susceptibility of the motors to the external force increases, the rates of motor state change can become greater than the friction timescale m/γ, crossing into the underdamped regime.

In the following, we focus on the properties of a commonly measured characteristic of the motion of tracer particles in experimental systems—the van Hove correlation function $P[\Delta x(\Delta t)]$. It is defined as the distribution of particle displacements $\Delta x \equiv x(t+\Delta t) - x(t)$ over a lag time Δt.

III. QUALITATIVE BEHAVIOR OF THE VAN HOVE DISTRIBUTION

Two qualitative behaviors of the VHD of tracer particle displacements have been observed in active gels: Gaussian [9] and exponential tails [6–8]. Both behaviors can be explained within the model defined above, in different regimes of the bulk elasticity, the number of motors, and the lag time Δt.

If a tracer particle is far enough from all active motors, its motion is caused by thermal noise combined with the small effect of each of the distant motion of many motors. In this case, its VHD will be Gaussian, irrespective of the value of k [14].

Exponential tails, as were observed in active gels [6–8] and living cells [37–40], can result from forces applied by a few nearby motors (as suggested in Ref. [6]) if the local bulk elasticity is small. In Appendix A, we show that within our model, in the limit of small bulk elasticity and small duty cycle (ratio of time in which a motor is on) $p_{\text{on}} \equiv \frac{k_{\text{on}}}{k_{\text{on}}+k_{\text{off}}}$, the exponential statistics of the motor active burst duration results in exponential tails of the VHD. For vanishing bulk elasticity $k = 0$, we prove that for a large enough Δx, $P(\Delta x) \propto e^{-\beta|\Delta x|/s}$, where $1/2 < \beta < 1$ and $s = F_0 \gamma^{-1} k_{\text{off}}^{-1}$. In numerical simulations of the model in the weak confinement regime $k/\gamma \ll k_{\text{off}}, k_{\text{on}}$, with a small but nonzero k, the VHD indeed displays exponential tails (Fig. 1). At short enough timescales, for small motor number N the VHD has peaks resulting from sampling of motion at nearly constant velocity during the entire sample time. Then, as Δt grows, exponential tails become evident until finally, at long enough times, the distribution is Gaussian nearly throughout the sampled domain of Δx values. Thus the model is consistent with observations of exponential tails in active gels.

A third behavior was predicted theoretically in Ref. [14] to occur within an experimentally relevant regime: if a tracer particle is in an environment with large bulk elasticity and

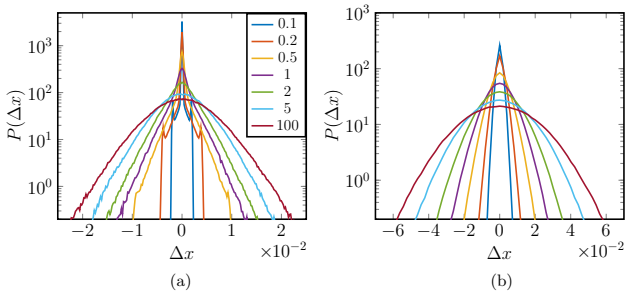

FIG. 1. Exponential tails in the weak confinement $k/\gamma \ll k_{\text{off}}, k_{\text{on}}$ and small p_{on} limits. The van Hove distribution is plotted for varying lag times Δt, for $k = 10$, $\gamma = 50$, $k_{\text{on}} = 1$, $k_{\text{off}} = 10$: (a) $N = 1$ and (b) $N = 10$.

in the vicinity of only a few motors, then side peaks appear in the long-time VHD [Figs. 2(a) and 2(b)], while at shorter times these peaks become shoulders [Figs. 2(c) and 2(d)]. Note that these side peaks which result from the balance between the active force and the restoring elastic force of the gel have so far not been observed in active-gel experiments. In Appendix B we estimate the values of the model parameters that appear in the experiments with respect to the regime where such side peaks should appear. In the next section we investigate the dependence of this peak structure on the properties of the active sources.

IV. VAN HOVE DISTRIBUTION PEAK RATIO

In the strong confinement limit $k_{\text{off}}, k_{\text{on}} \ll k/\gamma$, the steady-state particle position distribution $P(x)$ has sharp peaks

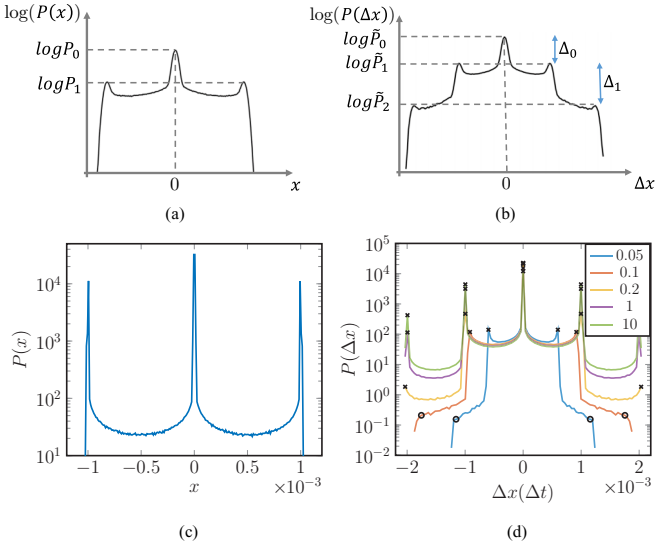

FIG. 2. (a) Sketch of the steady-state position distribution of the particle for $N = 1$ motor with the peak notations marked. (b) Sketch of the matching long-time VHD of particle displacements ($P[\Delta x(\Delta t \to \infty)]$). Notation for the distribution peaks and consecutive peak differences is marked. (c) The steady-state particle position distribution for $N = 1$ adamant motor ($k_{\text{on}} = 0.43$, $k_{\text{off}} = 1$, $k = 1000$, $F_0 = 1$, $\gamma = 50$). (d) The VHD for the same system as in (c). Different colors represent different lag times Δt. Detected peaks are marked by black x's and shoulders by black circles.

located at positions where the motor force is balanced by the harmonic potential force [14]. This is because the particle spends most of the time at the peaks of $P(x)$. Since the peaks are located at positions where the elastic force is balanced by the motor force, the distance between adjacent peaks is $x_0 \equiv F_0/k$. Therefore in order to observe peaks in experiments, in addition to the lower bound on k given by the strong confinement requirement above, there is also an upper bound on k requiring that $x_0 = F_0/k$ is larger than the spatial resolution of the measurement of the tracer position.

The overdamped Langevin equation governing the motion of the particle in the limit where the friction coefficient γ is larger than all other rates in the system is

$$\gamma \dot{x} = -kx - \sum_{i=1}^{N} M_i F_0. \tag{2}$$

The solution of this equation for a given constant $\sum_{i=1}^{N} M_i = N_{+1} - N_{-1} \equiv \Delta N$ is $x(t) = [x(0) - \Delta N F_0/k]\exp(-k/\gamma t) + \Delta N F_0/k$. Thus the typical timescale it takes the particle to reach the position corresponding to zero total force on it at a certain motor state is γ/k. When $k_{\text{off}}^{-1}, k_{\text{on}}^{-1} \gg \gamma/k$ the particle moves between the peaks of $P(x)$ much faster than the motor state changes, and therefore it spends much more time in the zero force positions of the motor states than moving between them. We will hence also refer to this limit as the fast particle limit.

$P(x)$ then has one central peak at $x = 0$ and $2N$ side peaks N on each side of $x = 0$ [Fig. 2(a)]. The long-time VHD is simply a self-convolution of $P(x)$: $P[\Delta x(\Delta t \to \infty)] = P(x) * P(x)$. Thus it has one central peak and $4N$ side peaks. Denote the value of $P(\Delta x)$ in each of the peaks $\tilde{P}_i$, where $i = -2N, -2N+1, \ldots, 2N$. In order to quantify the peak structure of the VHD, we measure the ratio of consecutive peak height differences in log scale [Fig. 2(b)]. The system is reflection symmetric and therefore $\tilde{P}_{-i} = \tilde{P}_i$. Thus for convenience we can focus without loss of generality on the peaks with non-negative indexes, which are at non-negative x values. We define the consecutive peak height differences in log scale: $\Delta_i = \log(\tilde{P}_i/\tilde{P}_{i+1})$. We study the dependence of the ratio of two consecutive log peak height differences, $r_i(\Delta t) = \Delta_i/\Delta_{i+1}$, on our model parameters and show that its value can be a signature of motor susceptibility to external force.

We begin by analyzing adamant motors, where the dynamics of the active sources do not depend on the stress in the gel and the rates k_{on}, k_{off} are constant. In Appendix C, we show that when $p_{\text{on}} \to 0$, the long-time VHD has $r_i \to 1$. Furthermore, $r_i < 1$ and quite close to 1 for all $p_{\text{on}} < p_{\text{on}}^c$ for $p_{\text{on}}^c \approx 0.6$ [Figs. 3(a) and 9]. Thus p_{on} needs to be larger than p_{on}^c in order to obtain $r_i > 1$. Moreover, numerical simulations (see details in Appendix D) show that this remains true for small Δt values (Figs. 3 and 4) in a sense that is clarified below. As Δt becomes smaller, the VHD becomes narrower, as the displacements are smaller over shorter times. Eventually, peaks [maximum points of $P(\Delta x)$] become shoulders [Fig. 2(d)]. A shoulder is a region of decreased slope between two regions with a larger slope. We define the location of the shoulder to be the minimum point of $|P'|$. As Δt decreases, $P(\Delta x)$ continuously deforms until there is no longer a maximum point where $P' = 0$ and instead $|P'| > 0$ throughout the region. This happens since the tracer does not have time to reach the force balance position, and remain there, within time Δt. When a peak $\tilde{P}_i$ becomes a shoulder as Δt decreases, we continue to use the notation $\tilde{P}_i$ for the shoulder point height.

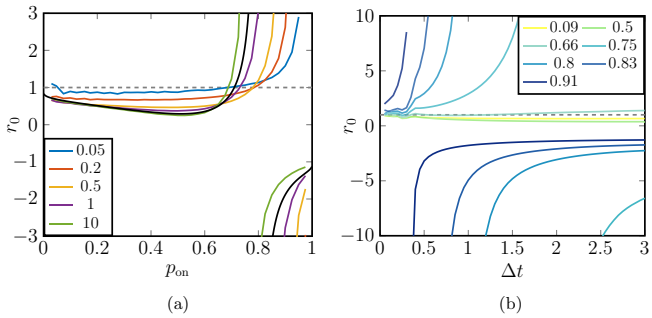

FIG. 3. r_0 in simulations with $N = 1$ adamant motor, $k_{\text{off}} = 1$, and varying k_{on} ($k = 1000$, $F_0 = 1$, $\gamma = 50$): (a) r_0 vs p_{on}. Different colors represent different lag times Δt. The black line is the approximate theoretical result for the fast particle limit at long lag times. (b) r_0 vs Δt. Colors represent different p_{on} values. For $p_{\text{on}} \lesssim 0.6$, $r_0 < 1$ at all lag times.

V. SUSCEPTIBLE MOTORS

Next, we study the model when the active sources are susceptible to external force. While the susceptibility of molecular motors, which are the source of activity in active gels, is a known phenomenon [15–20], it is not obvious how to take it into account in our model due to several reasons. First, because the precise nature of the active events that

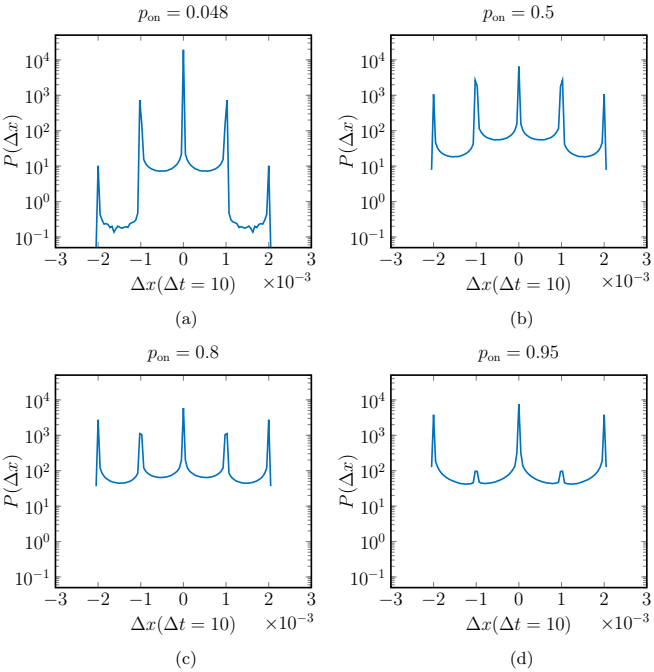

FIG. 4. (a)–(d) Long-time VHD for several simulations used to make Fig. 3, for varying k_{on} values at constant k_{off}. As p_{on} increases, the $i = 2$ peaks increase until passing the $i = 1$ peaks.

affect the tracer particle position in the active gel is unknown [6,9]. Second, because molecular motors respond to the force which acts on them locally, and it is unclear what this force is within our model, which does not assign a spatial position to the motors. We make the simple assumption that each of the motors is susceptible to the elastic force acting on the tracer particle, since this force is an indicator of the local stress in the gel. This means that the stochastic dynamics of the motor state variables M_i are now coupled to the particle position x, i.e., the motor state transition rates are functions of x. We therefore define $k_{\rm on}^{\pm}(x)$ to be the rate of transition from the off-state to the on-state in the $\pm$ direction, and $k_{\rm off}^{\pm}(x)$ to be the rate of transition from the on-state in the $\pm$ direction to the off-state.

In general, solving the coupled dynamics of the particle position and motor states to find $P(x)$ is difficult. We can solve it approximately in the fast particle limit $\gamma k_{\rm off,on}/k \ll 1$. Let us first consider the case of a single motor, $N = 1$. In this case, the steady-state particle density has three peaks at 0 and $\pm x_0$, for $x_0 = F_0/k$. In this limit the particle spends a small amount of time at positions that are not $x = 0, \pm x_0$. Thus we neglect all other states and treat the system as if it has three possible states, defined by the motor states $M = 0, \pm 1$, which correspond to a unique particle position $x = 0, \pm x_0$. We generally assume that the rate of transition between two states can depend on the current x and the nonzero M state involved (which could be the M value associated with the state from or into which the transition occurs) and denote the rates of transitions between these states as follows:

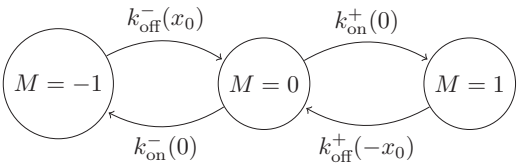

Assume that the rates depend only on $MF_{\rm elastic} = -Mkx$. Thus the system is symmetric to reflection of $x \to -x$ $M \to -M$. Therefore $k_{\rm on}^{-}(0) = k_{\rm on}^{+}(0) \equiv k_{\rm on}(0)/2$, and $k_{\rm off}^{+}(x_0) = k_{\rm off}^{-}(-x_0) \equiv k_{\rm off}(\pm x_0)$. The master equations for the system are as follows:

$$\begin{aligned}
\partial_t P(-x_0) &= \frac{k_{\rm on}(0)}{2} P(0) - k_{\rm off}(-x_0) P(-x_0) \\
\partial_t P(x_0) &= \frac{k_{\rm on}(0)}{2} P(0) - k_{\rm off}(x_0) P(x_0) \qquad (3) \\
\partial_t P(0) &= -k_{\rm on}(0) P(0) + k_{\rm off}(-x_0) P(-x_0) + k_{\rm off}(x_0) P(x_0).
\end{aligned}$$

The steady-state solution of the Eq. (3) is thus $P(x_0) = P(-x_0) = \frac{k_{\rm on}(0)}{2k_{\rm off}(x_0)} P(0)$.

The dimensionless ratio $k_{\rm on}(0)/k_{\rm off}(x_0)$ controls the steady-state distribution. Thus the particle position distribution and therefore the long-time VHD are approximately affected only by tuning the susceptibility (x dependence) of $k_{\rm off}$ and are indifferent to the dependence of $k_{\rm on}$ on the external force (since at $x = 0$ the external force is zero), as is evident in Figs. 5(b) and 5(d). At shorter times [Figs. 5(a) and 5(c)], this is not true since events where the motor turns on before reaching $x = 0$, with $k_{\rm on}$ that is dependent on the location x, can become dominant. For example, for a Δt close to

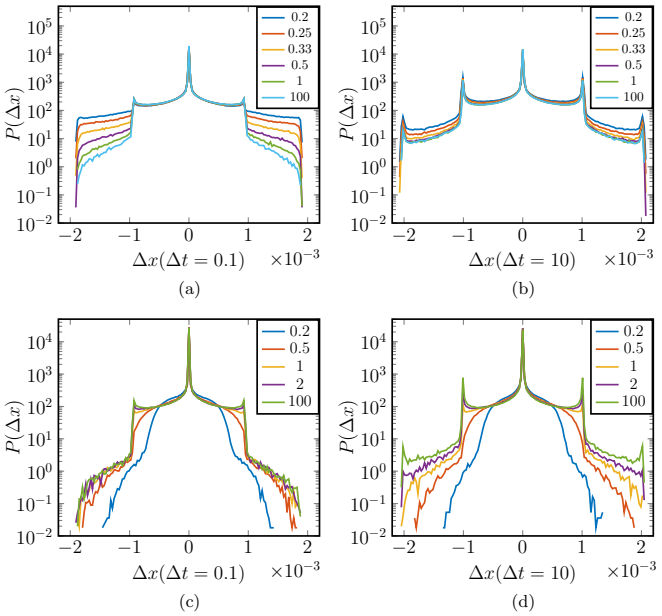

FIG. 5. Comparison of systems of $N = 1$ susceptible motor with susceptibility in the on or off rate. The VHD for various F_1 values is plotted for (a), (b) $k_{\rm on}^{\pm} = e^{\mp kx/F_1}$, $k_{\rm off} = 10$, for lag times of $\Delta t = 0.1$ (a) and $\Delta t = 10$ (b). For $\Delta t = 0.1$, increasing the susceptibility (decreasing F_1) increases the height of the shoulder $\tilde{P}_2$ and therefore increases r_0. (c), (d) $k_{\rm on} = 1$, $k_{\rm off} = 10e^{-Mkx/F1}$, for lag times of $\Delta t = 0.1$ (c) and $\Delta t = 10$ (d). Increasing the susceptibility causes peaks to become shoulders and move to smaller $|x|$. It does not increase $\tilde{P}_2$ or r_0. ($k = 1000$, $F_0 = 1$, $\gamma = 50$.)

the time it takes the particle to move from x_0 to $-x_0$ with $M_1 = -1$, $P(\Delta x = 2x_0)$ is a result of events where the motor state changed from $+1$ to 0 and nearly immediately to -1. The probability of such events depends on $k_{\rm on}^{\pm}(x)$.

The simplest possibilities are that either the active event rate $k_{\rm on}^{\pm}$ is susceptible to external force and the average event duration $1/k_{\rm off}^{\pm}$ is constant, or vice versa. We considered both of these options, with the assumption that the dependence of the rates on the elastic force is exponential and such that the motor force tends to align with the elastic force. We define the two models we study as follows:

(1) $k_{\rm off} = {\rm const}$, $k_{\rm on}^{\pm} = k_{\rm on}^{0} e^{\mp kx/F_1}$, where $k_{\rm on}^{0}$ is the basal on rate in the absence of forces and F_1 is a force scale that determines the sensitivity of the motors to external force. When $F_1 \to \infty$, the motors are adamant: $k_{\rm on}^{+} = k_{\rm on}^{-} = k_{\rm on}^{0}$, and each motor is equally likely to push to the left or to the right, regardless of the elastic force on the particle. In the infinite susceptibility limit $F_1 \to 0$, for $x > 0$: $k_{\rm on}^{+} \to 0$, $k_{\rm on}^{-} \to \infty$ and the motor turns on in the direction of the elastic force infinitely fast.

(2) $k_{\rm on} = {\rm const}$, $k_{\rm off} = k_{\rm off}^{0} e^{-Mkx/F1}$. In the adamant motor limit $F_1 \to \infty$: $k_{\rm off}^{+} = k_{\rm off}^{-} = k_{\rm off}^{0}$, and the motor is equally likely to turn off whether it is pushing with or against the elastic force. In the infinite susceptibility limit $F_1 \to 0$, for $x > 0$: $k_{\rm off}^{-} \to 0$, $k_{\rm off}^{+} \to \infty$, and the motor immediately turns off if it is pushing against the elastic force, and never turns off if it is pushing with the elastic force.

Since in experiments using actomyosin active gels the duty cycle of the active sources is likely small [2,6,9,14], we would like to explore the peak structure obtained in this regime.

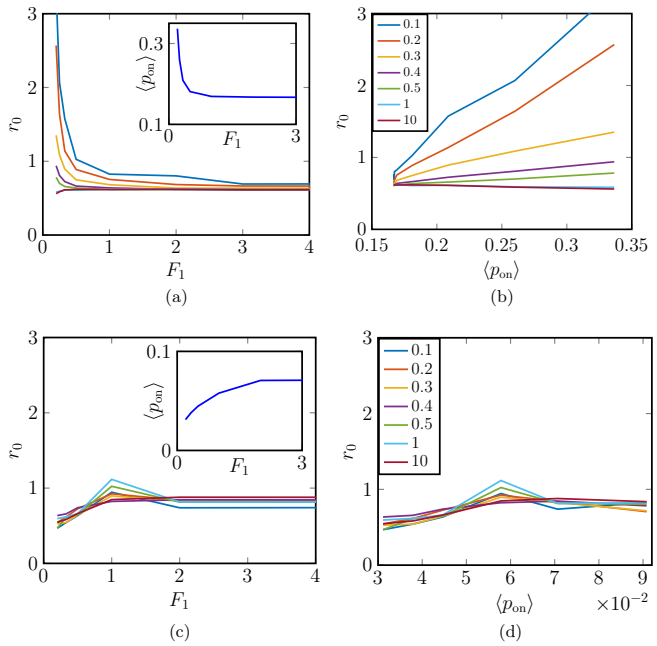

FIG. 6. The effect of susceptibility on r_0. For $k_{\rm on}^{\pm} = e^{\mp kx/F_1}$, $k_{\rm off} = 10$, $N = 1$: (a) r_0 as a function of F_1 for various lag times Δt. Inset: The average duty cycle $\langle p_{\rm on}\rangle$ as a function of F_1. (b) r_0 as a function of the average duty cycle $\langle p_{\rm on}\rangle(F_1)$ for various lag times Δt. For a small enough Δt, $r_0 > 1$ for much smaller $p_{\rm on}$ than in the adamant motor system. (c), (d) Same as (a) and (b) for $k_{\rm on} = 1$, $k_{\rm off} = 10e^{-Mkx/F1}$ ($k = 1000$, $F_0 = 1$, $\gamma = 50$).

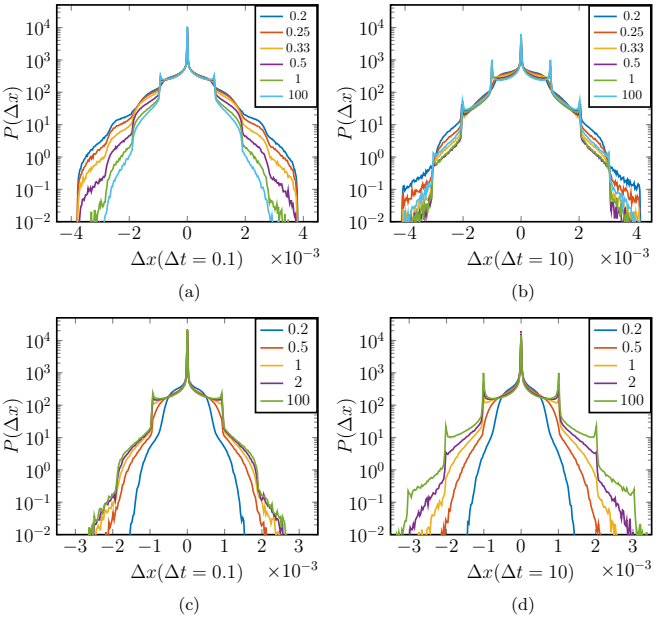

FIG. 7. Comparison of systems of $N = 2$ susceptible motor with susceptibility in the on or off rate. The van Hove distribution for various F_1 values is plotted for (a), (b) $k_{\rm on}^{\pm} = k_{\rm on}^{0} e^{\mp kx/F_1}$, $k_{\rm off} = 10$, for lag times of $\Delta t = 0.1$ (a) and $\Delta t = 10$ (b). Visibly, for the short lag time $\Delta t = 0.1$, increasing the susceptibility (decreasing F_1) increases the height of the shoulder $\tilde{P}_2$ and therefore increases r_0. (c), (d) $k_{\rm on} = 1$, $k_{\rm off} = 10e^{-Mkx/F1}$, for lag times of $\Delta t = 0.1$ (c) and $\Delta t = 10$ (d). Increasing the susceptibility causes peaks to become shoulders and move to smaller $|x|$. It does not increase $\tilde{P}_2$ or r_0. ($k = 1000$, $F_0 = 1$, $\gamma = 50$.)

Specifically, since in the small $p_{\rm on}$ regime we find $r_0 < 1$ for adamant motors, we would like to find if susceptibility of the active sources can result in $r_0 > 1$ even at a small average duty cycle (note that for susceptible motors the average duty cycle is a result of the system dynamics).

From numerical simulations, we find that a susceptible $k_{\rm off}$ does not increase r_0 above 1 [for $N = 1$ see Figs. 5(c), 5(d), 6(c), and 6(d); for $N = 2$ see Figs. 7(c), 7(d), 8(c), and 8(d)]. On the other hand, a susceptible $k_{\rm on}$ causes r_0 to be greater than 1 at smaller $p_{\rm on}$ values than that for adamant motors [for $N = 1$ see Figs. 5(a), 5(b), 6(a), and 6(b); for $N = 2$ see Figs. 7(a), 7(b), 8(a), and 8(b)].

VI. DISCUSSION

We considered a model for the motion of a tracer particle in an elastic gel due to active force sources of a typical force magnitude. We find that the two experimentally observed behaviors of the VHD of the tracer position displacements in actomyosin gels, Gaussian [9] and exponential tails [6–8], can be obtained in our model for different parameter values. Additionally, we explored the structure of side peaks in the VHD, which are predicted to occur in the limit of strong confinement ("fast particle") $k_{\rm off}, k_{\rm on} \ll k/\gamma$. We characterized the peak structure using the difference between adjacent peaks. We showed that for adamant motors, the ratio of the first two differences r_0 is larger than 1 only for large $p_{\rm on}$ values. When the active event rate is susceptible to the elastic stresses in the gel (which are quantified by the force on the tracer) such that the motor and elastic force tend to align, we find that $r_0 > 1$ is obtained even when the average duty cycle is small. When the active event duration is susceptible to the elastic stress, r_0 is not increased by the susceptibility.

The dynamics of a tracer particle inside active gels has not been explored yet in the regime in which we expect the side-peak structure of the VHD to appear: low density of active motors, and high elastic confinement. Our analysis of the side-peak structure of the VHD demonstrates that the details of this structure may serve as a sensitive probe to extract the correlations between the activity of neighboring motors. Note that the analysis we present is of a highly simplified "toy model," in one dimension, which does not have the full complexity of a cross-linked biopolymer network. More detailed simulations of such networks (such as [12]) could in the future incorporate motor-motor elastic interactions, as we introduced here. Our model may be potentially more generally useful, as it can be realized wherever a particle is driven by active forces within a confining potential. Such a situation can arise for cells within tissues, bacteria swarms, or artificial (nonbiological) systems.

ACKNOWLEDGMENTS

We thank Yair Shokef, Yael Roichman, Anne Bernheim, and Stanislav Burov for useful discussions. N.S.G. is the incumbent of the Lee and William Abramowitz Professorial Chair of Biophysics and this research was made possible in part by the generosity of the Harold Perlman family. N.S.G.

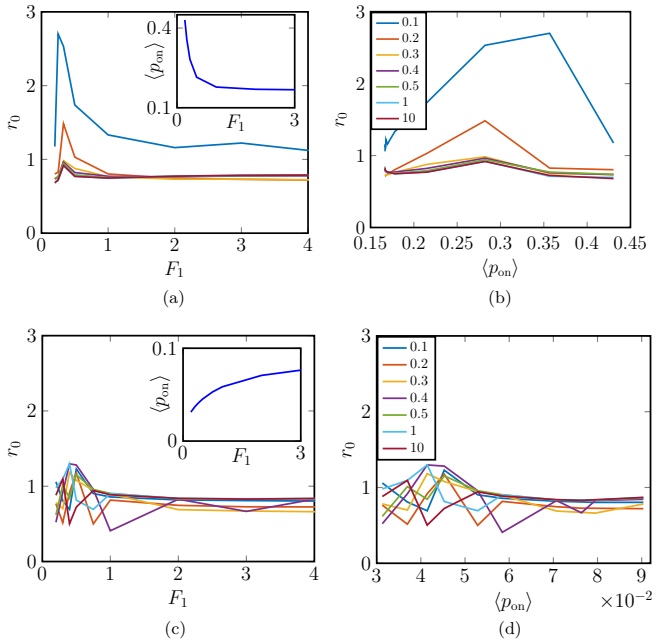

FIG. 8. The effect of susceptibility of the active event occurrence rate k_{on}. For the model with $k_{on}^{\pm} = e^{\mp kx/F_1}$, $k_{off} = 10$, $N = 2$: (a) r_0 as a function of F_1 for various lag times Δt. Inset: The average time ratio in which the motor was on $\langle p_{on} \rangle$ as a function of F_1. (b) r_0 as a function of the average duty cycle $\langle p_{on} \rangle(F_1)$ for various lag times Δt. Note that for a small enough Δt, $r_0 > 1$ for much smaller p_{on} than in the adamant motor system. (c), (d) Same as (a) and (b) for $k_{on} = 1$, $k_{off} = 10e^{-Mkx/F1}$. ($k = 1000$, $F_0 = 1$, $\gamma = 50$.)

acknowledges support from the ISF (Grant No. 580/12). N.R. acknowledges support from the Kimmelman Center for Biomolecular Structure and Assembly.

APPENDIX A: EXPONENTIAL TAIL OF THE VAN HOVE DISTRIBUTION IN THE WEAK CONFINEMENT LIMIT

We prove below that in the limit of negligible bulk elasticity $k = 0$, the van Hove distribution for a particle pushed by adamant motors has exponential tails. We neglect thermal fluctuations and other white noise forces, and thus assume that the particle moves freely due to the motor forces only. Since $k = 0$, the particle displacement is a sum of independent contributions due to each of the motors. We assume in the calculation of the van Hove distribution below that there is one motor ($N = 1$), and the result for a general N can be obtained from the distribution for $N = 1$ by $P[\Delta x(\Delta t); N] = P[\Delta x(N\Delta t); N = 1]$.

We will call the displacement due to a single motor on duration a single step and denote the displacement due to the ith step x_i. The total displacement of the particle within a time Δt can thus be written as

$$\Delta x = x_0 + \sum_{i=1}^{n} x_i + x_{n+1}, \tag{A1}$$

where x_i for $i = 1, \ldots, n$ are all steps as defined above, and x_0 and x_{n+1} are the displacement caused by possible incomplete steps that begin at the beginning of Δt or end when it ends and are not due to a motor state change. We shall assume that Δt is large enough with respect to the average on time k_{off}^{-1} so that the contribution to Δx from incomplete steps is negligible: $\sum_{i=1}^{n} x_i \gg x_0, x_{n+1}$. [Note that this assumption is consistent with the fact that we are interested in the tail of $P[\Delta x(\Delta t)]$.]

Using the law of total probability, the van Hove distribution can be written as

$$P[\Delta x(\Delta t)] = \sum_{n=0}^{\infty} P[\Delta x(\Delta t)|n(\Delta t)] P_n[n(\Delta t)], \tag{A2}$$

where $P_n[n(\Delta t)]$ is the distribution of the number of steps n that occurred within Δt. We will now calculate $P[\Delta x(\Delta t)|n(\Delta t)]$, the distribution of the displacement $\Delta x \approx \sum_{i=1}^{n} x_i$ given the number of steps that occurred within $\Delta t, n$.

The magnitude of the steps $|x_i|$ is distributed exponentially with mean $v k_{off}^{-1}$, where $v = F_0/\gamma$ is the particle velocity due to one motor force. Since the sign of x_i is ± 1 with probability $1/2$, x_i are i.i.d Laplace distributed with the probability density function (PDF) $f(x_i) = \frac{1}{2s} e^{-|x_i|/s}$ for $s = v k_{off}^{-1}$. Thus the PDF of the sum of n such independent random variables $\Delta x = \sum_{i=1}^{n} x_i$ is [41]

$$P(\Delta x|n) = \frac{e^{-|\Delta x|/s}}{s(n-1)!2^n} \sum_{j=0}^{n-1} \frac{(n-1+j)!}{(n-1-j)!j!} \frac{(|\Delta x|/s)^{n-1-j}}{2^j}. \tag{A3}$$

This is an exponential multiplied by a polynomial as a function of Δx; therefore it has an exponentially decaying tail. It is now left to show that $P_n(n)$ decays fast enough that $P[\Delta x(\Delta t)]$ also has an exponentially decaying tail: it satisfies $\lim_{\Delta x \to \infty} \frac{\log P(\Delta x)}{\Delta x} = c$ for a constant $c < 0$.

By substituting Eq. (A3) into Eq. (A2), rearranging the summations, and shifting indices, we obtain

$$P(\Delta x) = \frac{e^{-|\Delta x|/s}}{s} \frac{1}{2} \sum_{m=0}^{\infty} \frac{1}{m!} \frac{1}{2^m} f(m) \left(\frac{|\Delta x|}{s} \right)^m, \tag{A4}$$

where

$$f(m) = \sum_{j=0}^{\infty} P_n(j+m+1) \frac{(2j+m)!}{j!(j+m)!} \frac{1}{2^{2j}}. \tag{A5}$$

Since $P(\Delta x)$ is equal to $e^{-|\Delta x|/s}$ times a series in $|\Delta x|/s$ with positive coefficients, which hence diverges as $|\Delta x| \to \infty$, then $P(\Delta x) > e^{-|\Delta x|/s}$ for a large enough n. If a constant C exists such that $\forall m\, f(m) < C$, then from Eq. (A4) we conclude that $P(\Delta x) < \frac{C}{2s} \exp(-|\Delta x|/2s)$. Hence overall, for a large enough Δx, $P(\Delta x) \propto e^{-\beta|\Delta x|/s}$, where $1/2 < \beta < 1$.

We will show that this is true in the limit of $p_{on} \ll 1$, where the number of steps n taken within Δt is Poisson distributed with mean $\lambda \equiv k_{on} \Delta t$: $P_n(n) = e^{-\lambda} \lambda^n / n!$. In this case

$$f(m) = e^{-\lambda} \sum_{j=0}^{\infty} \frac{(2j+m)!}{j!(j+m)!(j+m+1)!} \frac{\lambda^{j+m+1}}{2^{2j}}. \tag{A6}$$

This series converges for every m.

Define

$$g(m) = \frac{(2j+m)! \lambda^m}{j!(j+m)!(j+m+1)!} \tag{A7}$$

then

$$\frac{g(m)}{g(m+1)} = \frac{j+m+2}{\lambda}\left(1 - \frac{j}{2N+m+1}\right) > \frac{j+m+2}{2\lambda}, \tag{A8}$$

and therefore for $m > 2\lambda - 2$, regardless of j, $g(m)$ is a decreasing function. Therefore for such m, $f(m)$ is also a decreasing function. Thus $f(m)$ has a maximal value for some M such that $0 \geqslant M \geqslant 2\lambda - 2$, and hence $\forall m\, f(m) < f(M) \equiv C$.

APPENDIX B: ESTIMATION OF THE VALUES OF THE MODEL PARAMETERS IN THE EXPERIMENTS

We give here estimates of the values of the model parameters, as obtained from experiments, to assess the experiments with respect to the regime where side peaks should occur. Some of these numbers are not precisely known, and we give a rough estimate.

The Young modulus of the actomyosin gels [9,10] is in the range $Y \sim 0.1$–1 Pa, while the effective viscosity felt by a micron-sized bead is $\eta \sim 1 - 10 \times \eta_{\text{water}} \sim 10^{-3}$–$10^{-2}$ Pa s. Using these numbers we obtain that the effective spring constant is [38] $k \sim 6\pi aY$ (where $a \sim 1\ \mu$m is the bead radius), while the effective friction coefficient is $\gamma \sim 6\pi a\eta$. We therefore estimate the following rate: $k/\gamma \sim 10$–$1000\ \text{s}^{-1}$.

This should be compared to the timescale of the active "bursts," the events where the accumulated motor-driven stress is released as a "kick" that actively moves the bead. From [2] we estimate this timescale to be of order $\sim$10–100 ms, such that $k_{\text{off}} \sim 10$–$100\ \text{s}^{-1}$. Since the duty ratio of myosin-II motors is low but depends on the number of motor heads in the minifilaments, we expect k_{on} to be of the same order of magnitude as k_{off}. Overall, these active gels do not seem to be clearly in the strong confinement limit ($k_{\text{off}}, k_{\text{on}} \ll k/\gamma$) where side peaks should be distinctly observed.

We can also estimate the displacement $x_0 \equiv F_0/k$ at which there is a force balance between the motor and the elastic restoring force. The myosin-II force is $F \sim 1$–10 pN, so we estimate $x_0 \sim 0.1$–$1\ \mu$m. We can compare this number to the maximal mean squared displacement (MSD) observed for the beads in the experiments, of order $\sqrt{\text{MSD}} \sim 0.1 - 0.3\,\mu$m. The conclusion is, again, that the conditions of the experiments are marginal with respect to allowing observation of the side peaks in the VHD.

APPENDIX C: $P(x)$ AND THE LONG-TIME VAN HOVE DISTRIBUTION IN THE FAST PARTICLE LIMIT

In this section we work in the fast particle limit $\gamma k_{\text{off,on}}/k \ll 1$, where the particle moves quickly between the peaks of the steady-state distribution $P(x)$, which occur at positions where the motor force is balanced by the harmonic potential force. We use an approximation where we completely neglect the transition time between the peaks and thus identify each motor state with a unique position of the particle in space.

Each N motor state $\mathbf{M} = (M_1, M_2, \ldots, M_N) \in \{0, \pm 1\}^N$ corresponds to a position $x = x_0 \Sigma_{i=1}^N M_i$, with $x_0 = F_0/k$, which the particle will reach in that motor state given enough time. We assume (as is approximately correct in the fast particle limit) that once the motor state changes, the particle immediately moves to its corresponding force balance position. Under this assumption each of the $2N+1$ peaks of the steady-state particle position distribution are δ functions. Denote the probability of finding the particle in mx_0 by P_m. Denote by $N_{0,\pm 1}$ the number of M_i variables equal to $0, \pm = 1$ (the total number of motors is $N_{-1} + N_0 + N_{+1} = N$). Denote the steady-state ratio of time in which a single motor is on $p_{\text{on}} = k_{\text{on}}/(k_{\text{on}} + k_{\text{off}})$. Each time a motor turns on it randomly chooses a direction of ± 1, so the probability to find a motor in the ± 1 state is $\frac{1}{2}p_{\text{on}}$. The probability to find a single motor in the off-state is $p_{\text{off}} = 1 - p_{\text{on}}$. Thus the steady-state distribution of (N_{+1}, N_{-1}) is a trinomial distribution:

$$P(N_{+1}, N_{-1}) = \frac{N!}{N_{+1}!N_{-1}!(N - N_{-1} - N_{+1})!} \times \left(\frac{1}{2}p_{\text{on}}\right)^{N_{-1}+N_{+1}} p_{\text{off}}^{N-N_{-1}-N_{+1}}. \tag{C1}$$

Therefore the peaks of $P(x)$ are given by

$$P_j = P\left(\sum_{i=1}^N M_i = |j|\right) = \sum_{k=|j|}^N P(N_{+1} = k, N_{-1} = k - |j|). \tag{C2}$$

In the long-time limit, the van Hove distribution is equal to the convolution of the steady-state position distribution with itself: $P[\Delta x(\Delta t \to \infty)] = P(x) * P(x)$. It has $4N+1$ peaks, which we will denote $\tilde{P}_i$ for integer $-2N \leqslant i \leqslant 2N$, corresponding to particle positions $x = ix_0$. They are given by the discrete convolution

$$\tilde{P}_i = \sum_{j=-N}^N P_j P_{i-j}, \tag{C3}$$

where the P_j are given by Eq. (C2) for $-N \leqslant j \leqslant N$ and zero otherwise. We will now show that the long-time van Hove distribution for a system with N motors is equal to the steady-state position distribution for a system with $2N$ motors, i.e., $\tilde{P}_i(N) = P_i(2N)$.

Proof.

$$\begin{aligned} P_i(2N) &= P\left(\sum_{k=1}^{2N} M_k = i\right) \\ &\overset{(*)}{=} \sum_{j=-N}^N P\left(\sum_{k=1}^N M_k = j\right) P\left(\sum_{k=N+1}^{2N} M_k = i - j\right) \\ &= \sum_{j=-N}^N P_j P_{i-j} = \tilde{P}_i(N), \end{aligned} \tag{C4}$$

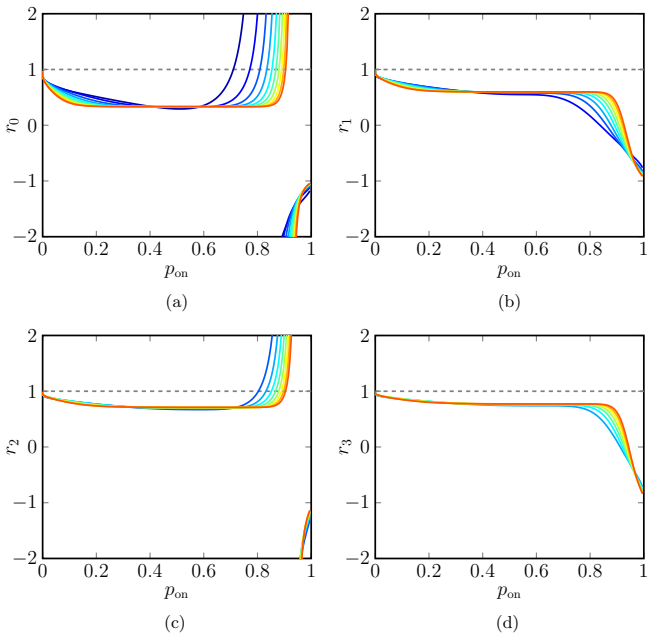

FIG. 9. (a)–(d) The results of the theoretical calculation of the long-time VHD peak ratio r_i for $i = 0$–3 in the fast particle limit [given by Eq. (C5) used in the definition of r_i]. Plots are for motor number $N = 1$–10, where the line color denotes the motor number and varies between dark blue ($N = 1$) and red ($N = 10$). Note $r_i \to 1$ as $p_{on} \to 0$, and $r_i < 1$ for $p_{on} \lesssim 0.6$ for all shown parameters.

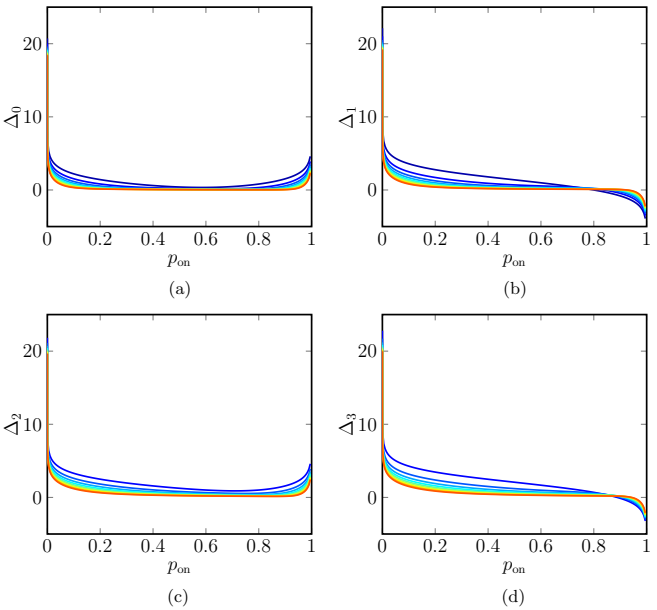

FIG. 10. (a)–(d) The results of the theoretical calculation of the long-time VHD peak difference Δ_i for $i = 0$–3 in the fast particle limit. Plots are for motor number $N = 1$–10 where the line color denotes the motor number and varies between dark blue ($N = 1$) and red ($N = 10$). Note that all the Δ_i are continuous and for even i positive, while for odd i cross zero.

where the equality (*) is due to the independence of the motor state variables M_i. Therefore

$$\begin{aligned}\tilde{P}_j(N) &= P_j(2N) \\ &= \sum_{k=|j|}^{2N} \frac{(2N)!}{k!(k-|j|)!(2N-2k+|j|)!} \\ &\quad \times \left(\frac{1}{2}p_{on}\right)^{2k-|j|} p_{off}^{2N-2k+|j|} \\ &= \frac{(2N)!}{|j|!(2N-|j|)!}\left(\frac{1}{2}p_{on}\right)^{|j|} p_{off}^{2N-|j|} + O\left(p_{on}^{|j|+2}\right).\end{aligned} \tag{C5}$$

Thus to leading order in small p_{on}, the distance between consecutive peaks of $P[\Delta x(\Delta t \to \infty)]$ in log scale is

$$\begin{aligned}\Delta_j &\equiv \log\left(\frac{\tilde{P}_j}{\tilde{P}_{j+1}}\right) \\ &\approx \log\left(\frac{p_{off}}{p_{on}}\right) + \log\left(\frac{j+1}{2N-j}\right).\end{aligned} \tag{C6}$$

For $p_{on} \to 0$, $\Delta_j \approx -\log(p_{on})$. Therefore in this limit the ratio of consecutive peak height differences $r_j \equiv \frac{\Delta_j}{\Delta j+1} \to 1$. A plot of r_j, calculated using Eq. (C5) (Fig. 9), reveals a stronger result: $r_j < 1$ for all $p_{on} < p_{on}^c$ for a rather large p_{on}^c. Thus p_{on} needs to be larger than p_{on}^c in order to obtain $r_j > 1$.

It may be noted that in Fig. 9 that at large p_{on} the r_i behave differently for odd and even i. While not directly relevant for our main point above, this behavior can be explained by the definitions of r_i and Δ_i, and Eq. (C5) for the value of $\tilde{P}_j(N)$. Figure 9 shows that for a large enough p_{on} the r_i become negative for all i. For even i, the r_i diverge when becoming negative, while for odd i the r_i do not diverge. This happens because the even Δ_i do not change sign and the odd ones do, as shown in Fig. 10. Since $r_i = \Delta_i/\Delta_{i+1}$, for odd i the denominator crosses zero while for even i the nominator does. When the motor duty cycle p_{on} increases, the outer side peaks height increases since the particle spends more time in the positions corresponding to more motors being on. If an outer side peak in the VHD becomes higher than the nearby inner one, the corresponding Δ_i becomes negative.

APPENDIX D: SIMULATION DETAILS

We performed simulations in which the Langevin equation of motion Eq. (1) was integrated using the Euler method. The particle steady-state position distribution and the van Hove displacement distribution for various lag times were estimated from the results by calculating a normalized histogram. Peaks and shoulders were automatically detected using algorithms that rely on the mathematical definition of peaks and shoulders but also using known features of the distributions our model produces in order to avoid false positives due to noise. Example results of the detection algorithm are plotted in Fig. 1(d).

Additional details about the simulation results are presented in figures. The results presented for each parameter set are from simulations with the following properties:

Figures 1(c), 1(d) and 2—Time difference between samples of the particle position: 0.05, total simulation run time: 10^6.

Figures 3, 4(a), and 4(b)—Time difference between samples of the particle position: 0.1, total simulation run time: 2×10^5.

Figures 4(c) and 4(d)–Time difference between samples of the particle position: 0.1, total simulation run time: 3×10^6.

Figure 5—Time difference between samples of the particle position: 0.1, total simulation run time: 10^5.

Figures 7 and 8—Time difference between samples of the particle position: 0.1, total simulation run time: (a), (b) 2×10^6 and (c), (d) 5×10^6.

The simulation step size was 10^{-4} in all of the simulations.

[1] F. Backouche, L. Haviv, D. Groswasser, and A. Bernheim-Groswasser, Phys. Biol. **3**, 264 (2006).

[2] D. Mizuno, C. Tardin, C. F. Schmidt, and F. C. MacKintosh, Science **315**, 370 (2007).

[3] M. E. Cates, S. M. Fielding, D. Marenduzzo, E. Orlandini, and J. M. Yeomans, Phys. Rev. Lett. **101**, 068102 (2008).

[4] F. C. MacKintosh and A. J. Levine, Phys. Rev. Lett. **100**, 018104 (2008).

[5] F. C. MacKintosh and C. F. Schmidt, Curr. Opin. Cell Biol. **22**, 29 (2010).

[6] T. Toyota, D. A. Head, C. F. Schmidt, and D. Mizuno, Soft Matter **7**, 3234 (2011).

[7] B. Stuhrmann, M. Soares e Silva, M. Depken, F. C. MacKintosh, and G. H. Koenderink, Phys. Rev. E **86**, 020901 (2012).

[8] M. S. e Silva, B. Stuhrmann, T. Betz, and G. H. Koenderink, New J. Phys. **16**, 075010 (2014).

[9] A. Sonn-Segev, A. Bernheim-Groswasser, and Y. Roichman, Soft Matter **13**, 7352 (2017).

[10] A. Sonn-Segev, A. Bernheim-Groswasser, and Y. Roichman, J. Phys.: Condens. Matter **29**, 163002 (2017).

[11] Y. Ideses, A. Sonn-Segev, Y. Roichman, and A. Bernheim-Groswasser, Soft Matter **9**, 7127 (2013).

[12] J. Alvarado, M. Sheinman, A. Sharma, F. C. MacKintosh, and G. H. Koenderink, Nat. Phys. **9**, 591 (2013).

[13] M. C. Marchetti, J. F. Joanny, S. Ramaswamy, T. B. Liverpool, J. Prost, M. Rao, and R. A. Simha, Rev. Mod. Phys. **85**, 1143 (2013).

[14] E. Ben-Isaac, E. Fodor, P. Visco, F. van Wijland, and N. S. Gov, Phys. Rev. E **92**, 012716 (2015).

[15] S. Klumpp and R. Lipowsky, Proc. Natl. Acad. Sci. USA **102**, 17284 (2005).

[16] T. Guérin, J. Prost, P. Martin, and J.-F. Joanny, Curr. Opin. Cell Biol. **22**, 14 (2010).

[17] S. Wang and P. G. Wolynes, Proc. Natl. Acad. Sci. USA **108**, 15184 (2011).

[18] S. Wang and P. G. Wolynes, Proc. Natl. Acad. Sci. USA **109**, 6446 (2012).

[19] M. C. Ucar and R. Lipowsky, Soft Matter **13**, 328 (2017).

[20] J. Sung, S. Nag, K. I. Mortensen, C. L. Vestergaard, S. Sutton, K. Ruppel, H. Flyvbjerg, and J. A. Spudich, Nat. Commun. **6**, 7931 (2015).

[21] N. Gov, Phys. Rev. Lett. **93**, 268104 (2004).

[22] P. Girard, J. Prost, and P. Bassereau, Phys. Rev. Lett. **94**, 088102 (2005).

[23] H. Turlier and T. Betz, arXiv:1801.00176.

[24] E. Ben-Isaac, Y. K. Park, G. Popescu, F. L. H. Brown, N. S. Gov, and Y. Shokef, Phys. Rev. Lett. **106**, 238103 (2011).

[25] D. Loi, S. Mossa, and L. F. Cugliandolo, Soft Matter **7**, 10193 (2011).

[26] A. Ghosh and N. Gov, Biophys. J. **107**, 1065 (2014).

[27] C. A. Weber, R. Suzuki, V. Schaller, I. S. Aranson, A. R. Bausch, and E. Frey, Proc. Natl. Acad. Sci. USA **112**, 10703 (2015).

[28] J. R. Gomez-Solano, L. Bellon, A. Petrosyan, and S. Ciliberto, Europhys. Lett. **89**, 60003 (2010).

[29] L. Berthier and J.-L. Barrat, Phys. Rev. Lett. **89**, 095702 (2002).

[30] D. Loi, S. Mossa, and L. F. Cugliandolo, Phys. Rev. E **77**, 051111 (2008).

[31] D. Loi, S. Mossa, and L. F. Cugliandolo, Soft Matter **7**, 3726 (2011).

[32] M. Wachsmuth, W. Waldeck, and J. Langowski, J. Mol. Biol. **298**, 677 (2000).

[33] S. C. Weber, A. J. Spakowitz, and J. A. Theriot, Proc. Natl. Acad. Sci. USA **109**, 7338 (2012).

[34] R. Bruinsma, A. Grosberg, Y. Rabin, and A. Zidovska, Biophys. J. **106**, 1871 (2014).

[35] A. Zidovska, Biophys. J. **108**, 540a (2015).

[36] A. Zidovska, Biophys. J. **112**, 180a (2017).

[37] P. Bursac, G. Lenormand, B. Fabry, M. Oliver, D. A. Weitz, V. Viasnoff, J. P. Butler, and J. J. Fredberg, Nat. Mater. **4**, 557 (2005).

[38] É. Fodor, M. Guo, N. S. Gov, P. Visco, D. A. Weitz, and F. van Wijland, Europhys. Lett. **110**, 48005 (2015).

[39] É. Fodor, V. Mehandia, J. Comelles, R. Thiagarajan, N. S. Gov, P. Visco, F. van Wijland, and D. Riveline, Biophys. J. **114**, 939 (2018).

[40] W. W. Ahmed, É. Fodor, M. Almonacid, M. Bussonnier, M.-H. Verlhac, N. Gov, P. Visco, F. van Wijland, and T. Betz, Biophys. J. **114**, 1667 (2018).

[41] S. Kotz, T. Kozubowski, and K. Podgorski, *The Laplace Distribution and Generalizations: A Revisit with Applications to Communications, Economics, Engineering, and Finance* (Springer Science & Business Media, New York, 2012).